

# Collective Quadrupole Excitations in the $50 < Z, N < 82$ Nuclei with the Generalized Bohr Hamiltonian

L. Próchniak, K. Zając and K. Pomorski

*Institute of Physics, The Maria Curie-Skłodowska University,  
pl. M. Curie-Skłodowskiej 1, 20-031 Lublin, Poland*

S. G. Rohoziński and J. Srebrny

*Department of Physics, Warsaw University,  
Hoża 69, 00-681 Warsaw, Poland*

## Abstract

The generalized Bohr Hamiltonian is applied to a description of low-lying collective excitations in even-even isotopes of Te, Xe, Ba, Ce, Nd and Sm. The collective potential and inertial functions are determined by means of the Strutinsky method and the cranking model, respectively. A shell-dependent parametrization of the Nilsson potential is used. An approximate particle-number projection is performed in treatment of pairing correlations. The effect of coupling with the pairing vibrations is taken into account approximately when determining the inertial functions. The calculation does not contain any free parameter.

## 1 Introduction

For many years the Generalized Bohr Hamiltonian (GBH) [1, 2, 3] has been still forming the only one model which, having possibilities to be derived microscopically (e.g. [4, 5, 6]), pretends to be able to describe collective excitations in the transitional nuclei or nuclei soft with respect to the quadrupole deformations. This is because the GBH is a scalar under rotations and, thus, possesses eigenstates of a good angular momentum whereas the most of other approaches deal with *intrinsic states* of an indefinite spin. Also, a rotation–vibration coupling, so important for transitional nuclei, is automatically taken into account in the Hamiltonian.

The aim of the present paper is to investigate the low-lying collective states in even–even nuclei from the region of  $50 < Z, N < 82$  within framework of the GBH. This region of the chart of nuclides is a good laboratory to study the collective model in its most general form as the standard approximations of it like the rotational and vibrational models are apparently not applicable to nuclei in question. Since the early calculation of

potential energy surfaces by Arseniev *et al.* [7] the  $50 < Z, N < 82$  nuclei are referred to as gamma-soft or susceptible to deformations leading to triaxial shapes. This is why the Wilets–Jean model was applied already long time ago to interpret experimental data [8]. On the other hand, the properties of these nuclides have been explained within the Davydov–Filippov model treating nuclei as rigid triaxial ones (cf. [9]). The triaxiality of the Xe and Ba isotopes has been discussed once more in the recent work of Meyer *et al.* [10]. Other theoretical approaches have also been applied to the investigated region. The closest to our study are the applications of Kumar’s dynamical deformation model to the Te nuclei [11] and the Frankfurt general collective model to the Ba isotopes [12]. Among methods different from ours we mention the microscopic calculations [13] of number- and spin-projected two-quasiparticle states with realistic interactions (MONSTER) and the Fermion Dynamical Symmetry Model [14], both applied to the Xe and Ba isotopes. The cranked Hartree–Fock–Bogolyubov calculations of the yrast bands and E2 properties have been performed for the Te and Xe isotopes [15, 16]. Within the Interacting Boson Model (IBM-1) the Xe and Ba nuclei have been treated in the SO(6) limit [17]. Also, the proton-neutron Interacting Boson Model (IBM-2) has been applied to the Xe, Ba and Ce isotopes [18]. We cite here only the newer papers on broader ranges of nuclides from the discussed region.

In Section 2 we recapitulate briefly the GBH recalling all necessary definitions and formulae. A new basis for the diagonalization of collective Hamiltonian is presented in Section 3. Some details of the basis construction are given in Appendix. To construct the collective Hamiltonian we use a standard microscopic model: nucleons in a deformed single particle potential interacting *via* the monopole pairing forces. We take the Nilsson potential with the parametrization of Seo [19] for a description of the single-particle motion. In treatment of the pairing forces we utilize an approximate projection technique based on the Generator Coordinate Method (GCM) for projecting the BCS wave function on the correct particle number [20]. Then, we calculate the collective potential by means of the Strutinsky macroscopic–microscopic method [21] and the inertial functions by means of the cranking model [4]. All the microscopic procedure is presented in Section 4. We know for a long time that the pairing correlations affect strongly the collective excitations. In early calculations for Xe and Ba isotopes we have decreased artificially the strength of the pairing interaction in order to simulate the coupling between the collective quadrupole and pairing vibrations [5]. Nowadays, when ampler data are available, we know that the effect cannot be approximated satisfactorily in that simple way. Sakamoto [22] has tried to remedy description of the collective states in xenon isotopes by including in a static way the quadrupole pairing interactions. We do believe that it is a dynamical effect. Here, we approximate the effect of coupling with the pairing vibrations by calculating the most probable dynamical value of the pairing energy gap as a function of deformation and putting it to microscopic calculations of the collective inertial functions. The procedure is discussed in Section 5. This way we have constructed the collective Hamiltonian and have solved it as it stands with no free parameters to be fitted. The results for the Te, Xe, Ba, Ce, Nd and Sm isotopes are presented in Section 6. Conclusions from our research are drawn in Section 7.

## 2 Recapitulation of the collective model

The five dynamical variables of the model constitute a quadrupole tensor and are usually denoted as  $\alpha_\mu$ ,  $\mu = -2, -1, \dots, 2$ . In order to separate rotations from vibrations, the variables  $\alpha$ 's are parametrized in terms of two deformation parameters,  $\beta$  and  $\gamma$  and three Euler angles,  $\phi, \theta, \psi$  (or  $\Omega$ , in short), defining the orientation of the intrinsic principal axes with respect to the laboratory frame:

$$\alpha_\mu = D_{\mu 0}^2(\Omega) \beta \cos \gamma + \frac{1}{\sqrt{2}} \left( D_{\mu 2}^2(\Omega) + D_{\mu -2}^2(\Omega) \right) \beta \sin \gamma, \quad (1)$$

where  $D_{\mu\nu}^\lambda(\phi, \theta, \psi)$  are the Wigner functions. Eq. (1) defines the intrinsic frame up to 24 rotations forming the octahedral group O [23, 24]. In consequence, only  $\beta$  is a unique function of  $\alpha$ 's. The remaining intrinsic variables undergo transformations of the group O.

The collective Hamiltonian, when expressed in terms of the intrinsic variables, is decomposed as

$$\hat{\mathcal{H}}_{\text{coll}} = \hat{\mathcal{T}}_{\text{vib}}(\beta, \gamma) + \hat{\mathcal{T}}_{\text{rot}}(\beta, \gamma, \Omega) + V_{\text{coll}}(\beta, \gamma), \quad (2)$$

where  $V_{\text{coll}}$  is the collective potential, the kinetic vibrational energy reads

$$\begin{aligned} \hat{\mathcal{T}}_{\text{vib}} = & -\frac{\hbar^2}{2\sqrt{wr}} \left\{ \frac{1}{\beta^4} \left[ \partial_\beta \left( \beta^4 \sqrt{\frac{r}{w}} B_{\gamma\gamma} \partial_\beta \right) - \partial_\beta \left( \beta^3 \sqrt{\frac{r}{w}} B_{\beta\gamma} \partial_\gamma \right) \right] + \right. \\ & \left. + \frac{1}{\beta \sin 3\gamma} \left[ -\partial_\gamma \left( \sqrt{\frac{r}{w}} \sin 3\gamma B_{\beta\gamma} \partial_\beta \right) + \frac{1}{\beta} \partial_\gamma \left( \sqrt{\frac{r}{w}} \sin 3\gamma B_{\beta\beta} \partial_\gamma \right) \right] \right\} \end{aligned} \quad (3)$$

and the rotational energy is

$$\hat{\mathcal{T}}_{\text{rot}} = \frac{1}{2} \sum_{k=1}^3 \hat{I}_k^2 / \mathcal{J}_k. \quad (4)$$

The mass parameters (or vibrational inertial functions) are denoted as  $B_{\beta\beta}$ ,  $B_{\beta\gamma}$  and  $B_{\gamma\gamma}$ . They are, in general, functions of  $\beta$  and  $\gamma$ . Moments of inertia  $\mathcal{J}_k$ , ( $k = 1, 2, 3$ ), in general also  $(\beta, \gamma)$ -dependent, are conventionally expressed by rotational inertial functions  $B_k$ :

$$\mathcal{J}_k = 4B_k(\beta, \gamma) \beta^2 \sin^2(\gamma - 2\pi k/3) \quad \text{for } k = 1, 2, 3. \quad (5)$$

The intrinsic components of total angular momentum are denoted as  $\hat{I}_k$ , ( $k = 1, 2, 3$ ). The determinants of the vibrational and rotational tensors are:

$$w = B_{\beta\beta} B_{\gamma\gamma} - B_{\beta\gamma}^2, \quad r = B_1 B_2 B_3. \quad (6)$$

The volume element has to have the form

$$d\tau = \beta^4 \sqrt{wr} |\sin 3\gamma| d\beta d\gamma d\Omega = \sqrt{wr} d\tau_0 \quad (7)$$

in order to fulfill the hermiticity condition for  $\hat{\mathcal{H}}_{\text{coll}}$ . The collective electromagnetic E2, M1 and E0 operators are determined by their  $(\beta, \gamma)$ -dependent intrinsic components in

the following way:

$$\begin{aligned}
\hat{\mathcal{M}}(\text{E2}; \mu) &= \sqrt{\frac{5}{16\pi}} \{ D_{\mu 0}^2(\Omega) Q_0(\beta, \gamma) \\
&\quad + \frac{1}{\sqrt{2}} (D_{\mu 2}^2(\Omega) + D_{\mu -2}^2(\Omega)) Q_2(\beta, \gamma) \}, \\
\hat{\mathcal{M}}(\text{M1}; \mu) &= \sqrt{\frac{3}{4\pi}} \{ D_{\mu 0}^1(\Omega) \mathcal{G}_3(\beta, \gamma) \hat{I}_3 \\
&\quad - \frac{1}{\sqrt{2}} (D_{\mu 1}^1(\Omega) - D_{\mu -1}^1(\Omega)) \mathcal{G}_1(\beta, \gamma) \hat{I}_1 \\
&\quad + \frac{i}{\sqrt{2}} (D_{\mu 1}^1(\Omega) + D_{\mu -1}^1(\Omega)) \mathcal{G}_2(\beta, \gamma) \hat{I}_2 \}, \\
\hat{\mathcal{M}}(\text{E0}) &= ZeR^2(\beta, \gamma).
\end{aligned} \tag{8}$$

Although the above description of the nuclear collective excitations is sometimes called *a geometrical model* it is needless at this stage to refer to the geometrical picture of nucleus. The model is just defined by seven functions of  $\beta$  and  $\gamma$ :  $V_{\text{coll}}$ , the collective potential and  $B_{\beta, \beta}$ ,  $B_{\beta, \gamma}$ ,  $B_{\gamma, \gamma}$ ,  $B_1$ ,  $B_2$ ,  $B_3$ , the inertial functions. To investigate electromagnetic properties additional functions should be defined, for instance,  $Q_0$  and  $Q_2$ , the quadrupole electric moments,  $\mathcal{G}_1$ ,  $\mathcal{G}_2$  and  $\mathcal{G}_3$ , the gyromagnetic functions and  $R^2$ , the square of electric radius, as presented in eq. (8) above. All of these 13 functions have to be determined from a microscopic theory. The geometry may conceivably be inherent in there.

### 3 The basis in the collective space

The methods used hitherto to solve the eigenvalue problem for Hamiltonian of eq. (2) can be divided into two groups. The former group consists in a direct numerical solution of a system of partial differential equations using finite difference methods [2, 5, 25]. The latter methods resolve themselves to matrix eigenvalue problems by means of expanding the eigenfunctions in a complete set of functions of  $\beta$ ,  $\gamma$ ,  $\phi$ ,  $\theta$ ,  $\psi$  [26, 27, 28, 29]. Then, the problem of construction of an appropriate basis for a given angular momentum arises. The five-dimensional oscillator wavefunctions of a good angular momentum constitute a natural basis [24, 30, 31, 32, 33].

Following the idea of Libert and Quentin we construct the basis [29] from a complete set of square integrable functions of  $\beta_0 = \beta \cos \gamma$ ,  $\beta_2 = \beta \sin \gamma$  and  $\Omega$  in the form of product of gaussians and monomials in  $\beta$ 's, and the Wigner function in  $\Omega$ :

$$e^{-\mu\beta^2/2} (\beta_0)^{n_0} (\beta_2)^{n_2} D_{ML}^I(\Omega) \tag{9}$$

for  $n_0, n_2 = 0, 1, \dots$ ,  $I = 0, 1, \dots$  and  $M, L = -I, \dots, I$ . This basis is equivalent to the set of functions

$$\varphi_{Lmn}^{IM}(\beta, \gamma, \Omega) = e^{-\mu\beta^2/2} \beta^n \begin{Bmatrix} \cos m\gamma \\ \sin m\gamma \end{Bmatrix} D_{ML}^I(\Omega) \tag{10}$$

with  $n = 0, 1, \dots$  and  $m = n, n-2, \dots, 0$  or 1. The functions  $\varphi_{Lmn}^{IM}(\beta, \gamma, \Omega)$  form a complete set of nonorthogonal, square integrable functions with respect to measure  $d\tau_0$ . The basis functions (10) depend on a parameter  $\mu$  which is to be chosen further. Then we symmetrize appropriately the functions  $\varphi$  of eq. (10) under the octahedral group O using a method close to that presented in ref. [34]. Details of the symmetrization procedure are

published elsewhere [35]. The O-invariant functions generated from the set of eq. (10) and forming a basis take the following form:

$$\tilde{\Psi}_{Lmn}^{IM}(\beta, \gamma, \Omega) = e^{-\mu\beta^2/2} \beta^n \sum_{K=\text{even} \geq 0} \tilde{f}_{LmK}^I(\gamma) \Phi_{MK}^I(\Omega) \quad (11)$$

with ranges of  $I$ ,  $M$ ,  $n$  and  $m$  given above. Quantum number  $L$  runs over natural even values within a range specific for given  $I$  and  $m$  [35]. The form of functions  $\tilde{f}_{LmK}^I(\gamma)$  and possible values of  $L$  are given in Appendix. The Euler angles dependence of  $\tilde{\Psi}$ 's is given through the Wigner functions:

$$\Phi_{MK}^I(\Omega) = \sqrt{\frac{2I+1}{16\pi^2(1+\delta_{K0})}} \left( D_{MK}^I(\Omega) + (-1)^I D_{M-K}^I(\Omega) \right) \quad (12)$$

The nonorthogonal basis of eq. (11) can be used to diagonalize Hamiltonian  $\hat{\mathcal{H}}_{\text{coll}}$  as, for instance, Kumar does [28]. Instead, we orthogonalize it applying Cholesky–Banachiewicz procedure [36] as is described in Appendix. In order to make the basis most effective the parameter  $\mu$  has to be chosen appropriately. The natural choice is to fit potential  $V_{\text{coll}}$  to a paraboloid of revolution with stiffness  $C$ , to take a mean value  $B$  of all of inertial functions and then to use the oscillator formula:

$$\mu = \left( \frac{BC}{\hbar^2} \right)^{1/4}. \quad (13)$$

We have tested the above choice of  $\mu$  and checked that it works fairly well. The maximal value of the order of the polynomial  $\beta^n$  in eq. (11) is fixed by the plateau condition. In our case it was  $n = 16$ .

## 4 The microscopic model

We describe microscopically the nucleus as a system of nucleons moving in a deformed mean field and interacting through monopole (state-independent) pairing forces. Thus, the microscopic Hamiltonian reads:

$$\hat{H} = \hat{H}_{\text{s.p.}} + \hat{H}_{\text{pair}} \quad (14)$$

with

$$\hat{H}_{\text{s.p.}} = \sum_{\nu>0} \langle \nu | \hat{h} | \nu \rangle (c_{\nu}^{\dagger} c_{\nu} + c_{-\nu}^{\dagger} c_{-\nu}), \quad (15)$$

$$\hat{H}_{\text{pair}} = - \sum_{t=\pm 1/2} G_t \sum_{\nu>0} \langle \nu | (\frac{1}{2} + t\tau_3) | \nu \rangle c_{\nu}^{\dagger} c_{-\nu}^{\dagger} \sum_{\nu'>0} \langle \nu' | (\frac{1}{2} + t\tau_3) | \nu' \rangle c_{-\nu'} c_{\nu'}, \quad (16)$$

where  $t = \pm 1/2$  is the isospin projection of neutron and proton, respectively. We use the Nilsson single particle Hamiltonian  $\hat{h}$  with the shell dependent parametrization [19] of the  $\mathbf{l}s$  and  $\mathbf{l}^2$  correction terms. Namely

$$v_{\mathbf{l}s} = -2\hbar\omega_0\kappa_{NI}\mathbf{l} \cdot \mathbf{s}, \quad (17)$$

$$v_{\mathbf{l}^2} = -\hbar\omega_0(\mu_{NI}\mathbf{l}^2 - \langle \mu_{NI}\mathbf{l}^2 \rangle_{\text{shell}}), \quad (18)$$

where

$$\kappa_{Nl} = \kappa_0[1 + 8\mu_{Nl}(N + 3/2)] + \kappa_1 A^{1/3} P_{s,Nl}, \quad (19)$$

$$\mu_{Nl} = \mu_0 P_{i,Nl}^2 \quad (20)$$

and  $P_{s,Nl}$ ,  $P_{i,Nl}$  are the following integrals (evaluated numerically) of the harmonic oscillator radial wave function  $R_{Nl}(r)$ :

$$P_{i,Nl} = \int_0^{R_0 - a/2} R_{Nl}^2(r) r^2 dr \quad (21)$$

$$P_{s,Nl} = \int_{R_0 - a/2}^{R_0 + a/2} R_{Nl}^2(r) r^2 dr \quad (22)$$

Here  $R_0$  and  $a$  stand for the nuclear radius and the surface thickness, respectively. We take, after ref. [19],  $\kappa_0 = 0.021$ ,  $\kappa_1 = 0.9$ ,  $\mu_0 = 0.062$  and we take  $A = 130$  as the average nuclear mass in the considered region.

When solving the eigenproblem of the pairing Hamiltonian  $\hat{H}_{\text{pair}}$  we replace the standard BCS formalism by an approximate projection of the BCS wave function on a given particle number [20]. This procedure is based on the gaussian overlap approximation (GOA) of the generator coordinate method (GCM) and gives results close to the exact projection. Moreover, the GCM projection is very convenient because its results are easy to present in terms of the usual BCS formalism. The form of BCS equations for the energy gap  $\Delta$  and the Fermi energy  $\lambda$  remains unchanged. The only effect of the particle number projection is that the standard BCS energy (of particles with isospin projection  $t$ )

$$V_{\text{BCS}}(\Delta) = \sum_{\nu > 0} (2e_\nu v_\nu^2 - G_t v_\nu^4) - \frac{\Delta^2}{G_t}, \quad (23)$$

is now corrected so as that the pairing energy is

$$V_{\text{pair}}(\Delta) = V_{\text{BCS}}(\Delta) - \left( \sum_{\nu > 0} \frac{(e_\nu - \lambda)(u_\nu^2 - v_\nu^2) + 2\Delta u_\nu v_\nu + G_t v_\nu^4}{E_\nu^2} \right) / \left( \sum_{\nu > 0} E_\nu^{-2} \right). \quad (24)$$

Here  $e_\nu$  is an eigenvalue of  $\hat{h}$  and  $v_\nu^2$ ,  $u_\nu^2 = 1 - v_\nu^2$  are the usual BCS occupation probabilities, and  $E_\nu = \sqrt{(e_\nu - \lambda)^2 + \Delta^2}$  is the quasiparticle energy. The  $2\sqrt{15}Z$  (or  $N$ ) levels closest to the Fermi surface were taken when solving the BCS equation. It was shown [37] that when the projection on a given particle number is performed the pairing strength parameter should be renormalized with respect to the standard value in order to get the proper energy gaps. With the estimation:

$$G_t = \begin{cases} g_0/(A-Z)^{2/3} & \text{for } t = 1/2, \\ g_0/Z^{2/3} & \text{for } t = -1/2 \end{cases} \quad (25)$$

where  $g_0 = 0.285 \hbar \omega_0$ , we can reasonably reproduce the experimental values of energy gaps. This is shown in Fig. 1 where experimental gaps deduced from measured or estimated [38] nuclear masses are compared with theoretical values of neutron gap  $\Delta_n$ .

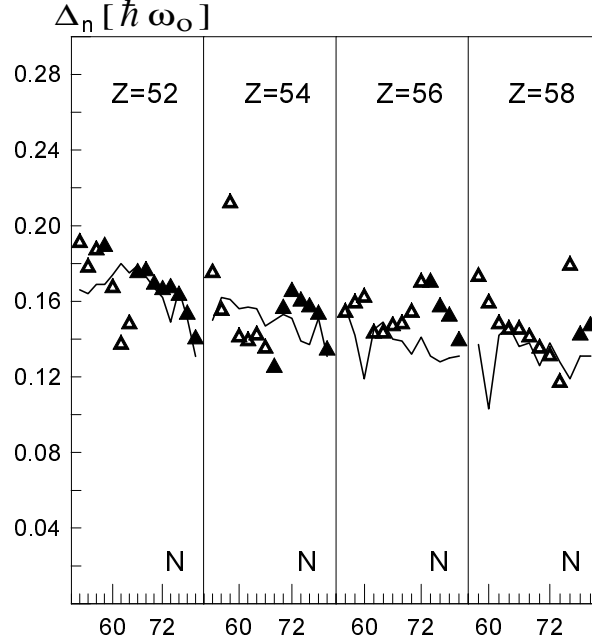


Fig. 1: The theoretical and experimental neutron energy gaps for isotopes of Te, Xe, Ba and Ce. Experimental points obtained from measured or estimated [38] nuclear masses are represented by full or open triangles, respectively. Theoretical values are marked with lines.

We apply the Strutinsky microscopic-macroscopic method [21] to calculate the collective potential and we use the cranking model for determining moments of inertia, gyromagnetic functions and vibrational inertial functions. The standard cranking formulae read [4, 5]:

$$\mathcal{J}_k = 2\hbar^2 \sum_{\nu, \nu' > 0} \frac{(u_\nu v_{\nu'} - u_{\nu'} v_\nu)^2}{E_\nu + E_{\nu'}} |\langle \nu | \hat{j}_k | \nu' \rangle|^2, \quad (26)$$

$$\mathcal{G}_k = \frac{2\hbar^2}{\mathcal{J}_k} \sum_{\nu, \nu' > 0} \frac{(u_\nu v_{\nu'} - u_{\nu'} v_\nu)^2}{E_\nu + E_{\nu'}} \langle \nu | \hat{j}_k | \nu' \rangle \langle \nu' | \hat{\mu}_k | \nu \rangle, \quad (27)$$

where  $\hat{j}_k$  and  $\hat{\mu}_k$  ( $k = 1, 2, 3$ ) are components of the single particle total angular momentum and magnetic moment, respectively, and

$$B_{qq'} = \frac{\hbar^2}{f(q)f(q')} \left\{ 2 \sum_{\nu, \nu' > 0} \frac{(u_\nu v_{\nu'} + u_{\nu'} v_\nu)^2}{(E_\nu + E_{\nu'})^3} \langle \nu | \frac{\partial \hat{h}}{\partial q} | \nu' \rangle \langle \nu' | \frac{\partial \hat{h}}{\partial q'} | \nu \rangle + \right. \\ \left. + \frac{1}{4} \sum_{\nu > 0} \frac{\Delta^2}{E_\nu^5} \left[ \frac{\partial \lambda}{\partial q} \frac{\partial \lambda}{\partial q'} - \left( \frac{\partial \lambda}{\partial q} \langle \nu | \frac{\partial \hat{h}}{\partial q'} | \nu \rangle + \frac{\partial \lambda}{\partial q'} \langle \nu | \frac{\partial \hat{h}}{\partial q} | \nu \rangle \right) \right] \right\} \quad (28)$$

for  $q, q' = \beta$  or  $\gamma$ , where  $f(\beta) = 1$ ,  $f(\gamma) = \beta$ . To be complete we quote at the end formulae for the electric moments:

$$Q_0 = Ze \sqrt{\frac{16\pi}{5}} \sum_{\nu > 0} 2v_\nu^2 \langle \nu | \frac{1}{2} (1 - \tau_3) r^2 Y_{20} | \nu \rangle, \quad (29)$$

$$Q_2 = Ze\sqrt{\frac{16\pi}{5}} \sum_{\nu>0} 2v_\nu^2 \langle \nu | \frac{1}{2}(1 - \tau_3) \frac{r^2}{\sqrt{2}} (Y_{22} + Y_{2-2}) | \nu \rangle , \quad (30)$$

$$R^2 = \sum_{\nu>0} 2v_\nu^2 \langle \nu | \frac{1}{2}(1 - \tau_3) r^2 | \nu \rangle . \quad (31)$$

## 5 Effect of the collective pairing vibrations

It is suspected for a long time [5, 39, 40] that the pairing vibrations are coupled to the collective quadrupole motion. Here we do not construct a complete "quadrupole + pairing" collective model which would have nine degrees of freedom and could not be easy to solve. We just take approximately into account the effect of the pairing vibrations on the quadrupole excitations in question.

The collective pairing Hamiltonian has the following structure [41, 42, 43]:

$$\begin{aligned} \hat{\mathcal{H}}_{\text{pair}} = & -\frac{\hbar^2}{2\sqrt{w_\Delta(\Delta)r_\Phi(\Delta)}} \frac{\partial}{\partial \Delta} \frac{\sqrt{w_\Delta(\Delta)r_\Phi(\Delta)}}{B_{\Delta\Delta}(\Delta)} \frac{\partial}{\partial \Delta} + \frac{\hbar^2}{2\mathcal{J}_\Phi(\Delta)} \hat{\mathcal{N}}^2 \\ & + A_{\text{pair}}(\Delta) \hat{\mathcal{N}} + V_{\text{pair}}(\Delta) \end{aligned} \quad (32)$$

where  $\hat{\mathcal{N}} = -i\partial/\partial\Phi$  is the particle number excess operator and  $\Phi$  is the gauge angle. Expressions for the functions  $B_{\Delta\Delta}(\Delta)$ ,  $\mathcal{J}_\Phi(\Delta)$ ,  $w_\Delta(\Delta)$ ,  $r_\Phi(\Delta)$  and  $A_{\text{pair}}(\Delta)$  obtained from GCM and GOA are given in ref. [42].

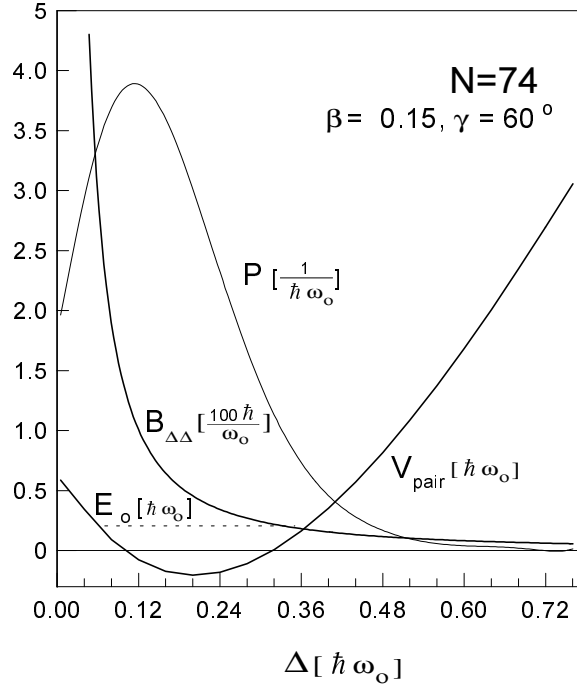


Fig. 2: The neutron zero-point pairing vibration at deformation  $\beta = 0.15$ ,  $\gamma = 60^\circ$  for neutron number  $N = 74$ . The equilibrium value of the energy gap  $\Delta_{\text{BCS}} \approx 0.20\hbar\omega_0$  while the most probable value  $\Delta_0 \approx 0.12\hbar\omega_0$ .



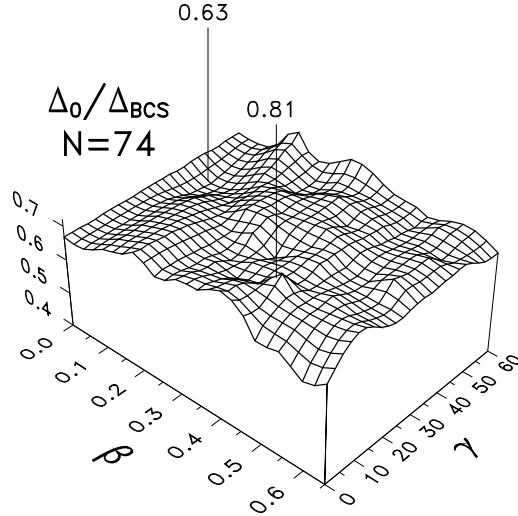


Fig. 3: Ratio of the neutron energy gaps  $\Delta_0/\Delta_{\text{BCS}}$  as a function of  $\beta$  and  $\gamma$  for the neutron number  $N = 74$ . The minimal and maximal values of the ratio are marked on the surface.

The ground-state energy,  $E_0$ , of the pairing vibrations is to be found from the following eigenvalue problem:

$$\hat{\mathcal{H}}_{\text{pair}}\Psi_0(\Delta) = E_0\Psi_0(\Delta), \quad \hat{\mathcal{N}}\Psi_0(\Delta) = 0, \quad (33)$$

which we solve at each deformation point  $(\beta, \gamma)$  for a given number  $N$  of neutrons or a given number  $Z$  of protons, respectively. This way we find  $E_0(\beta, \gamma)$  and  $\Psi_0(\Delta; \beta, \gamma)$  separately for neutrons and protons in a given nucleus. Then, we replace  $\Delta_{\text{BCS}}$  of the BCS (such that  $V_{\text{pair}}(\Delta) = \min$ ) in all collective functions (eqs (26), (27), (28) and (29)) by the most probable value of the energy gap  $\Delta_0$ , i.e. for which the probability

$$P(\Delta) = |\Psi_0|^2 w_{\Delta} r_{\Phi} \quad (34)$$

of finding a given value of  $\Delta$  in the ground state is maximal (Fig. 2). Since  $B_{\Delta\Delta}$  decreases rapidly with the increase of  $\Delta$ , the values of  $\Delta_0$  are systematically lower than the equilibrium energy gaps for all values of  $\beta$  and  $\gamma$  (cf. [40]). An example of such a behaviour is demonstrated in Fig. 3.

## 6 Results

The collective model in version presented in Section 2 with the Hamiltonian and electromagnetic multipole operators constructed in the framework of microscopic model discussed in Section 4 has been applied for a description of the collective states in even-even isotopes of Te, Xe, Ba, Ce, Nd and Sm. The effect of coupling with the pairing vibrations as reported in Section 5 has been taken approximately into account. The calculations have been performed with no free parameters to be fitted. The results are discussed below.

## 6.1 The energy spectra

The calculated energy levels in the six isotope chains in question are shown in Figs 4, 5, 6, 7, 8 and 9, respectively and compared with the experimental spectra which are taken from [44] unless another reference is quoted.

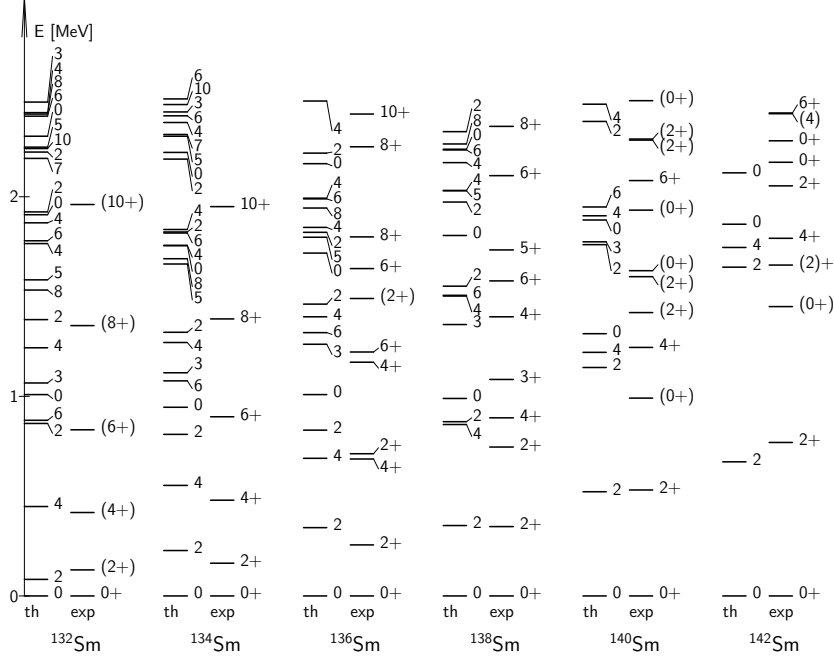


Fig. 4: Calculated (th) and experimental (exp) energy levels in the even-even samarium isotopes  $^{132-142}\text{Sm}$ . The theoretical levels are marked with spin (parity of all of states is positive), while the experimental ones — with spin and parity. Experimental data are taken from [44].

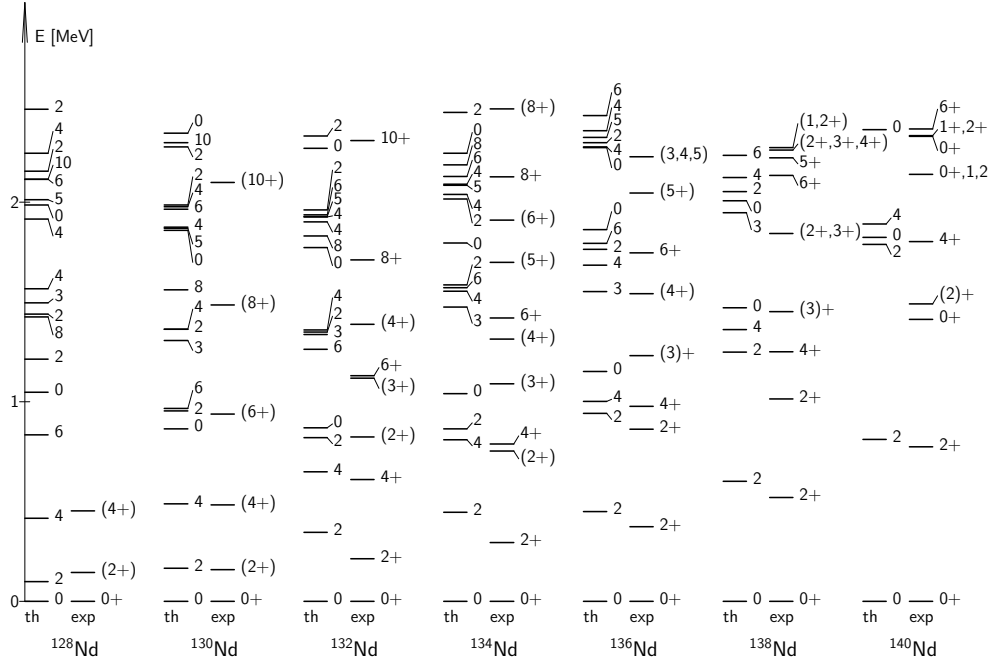


Fig. 5: The same as in Fig. 4 but for neodymium isotopes  $^{126-140}\text{Nd}$ .

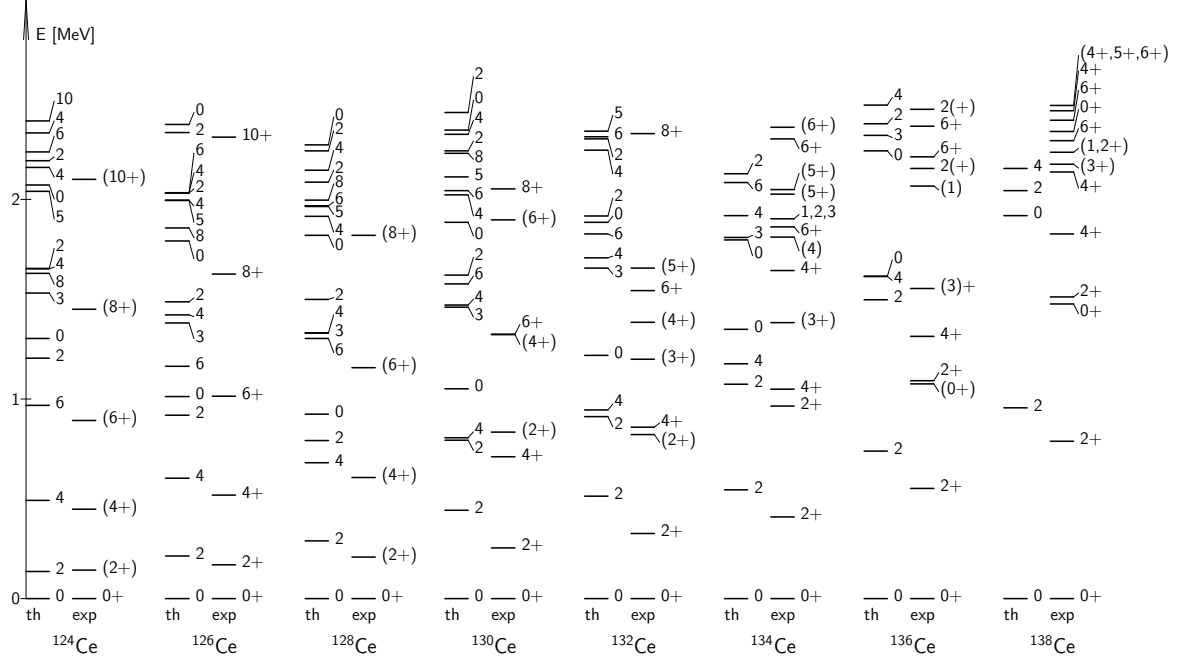


Fig. 6: The same as in Fig. 4 but for cerium isotopes  $^{124-138}\text{Ce}$ .

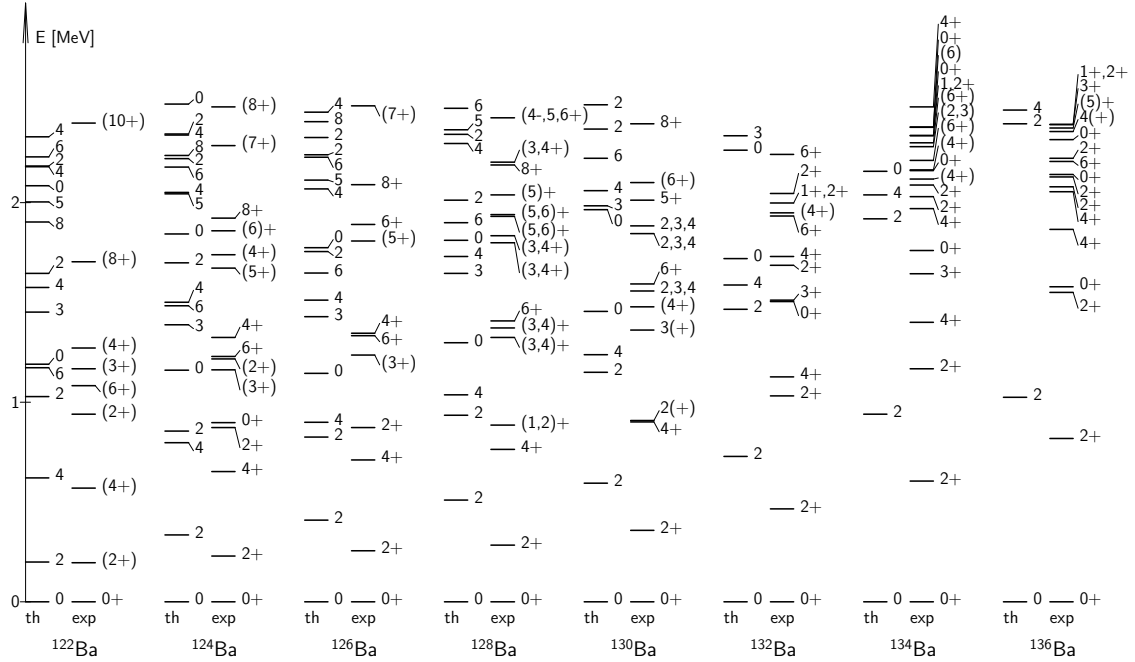


Fig. 7: The same as in Fig. 4 but for barium isotopes  $^{122-136}\text{Ba}$ .

The energy spectra in all of the isotopes of the two heaviest elements in question, Nd and Sm, are reproduced fairly well. The yrast states  $2^+$ ,  $4^+$ ,  $6^+$  and  $8^+$  and the second  $2^+$  state are in more or less correct positions, although the yrast bands are little bit too stretched (Figs 4 and 5). Similar results we have got for three lightest cerium isotopes,

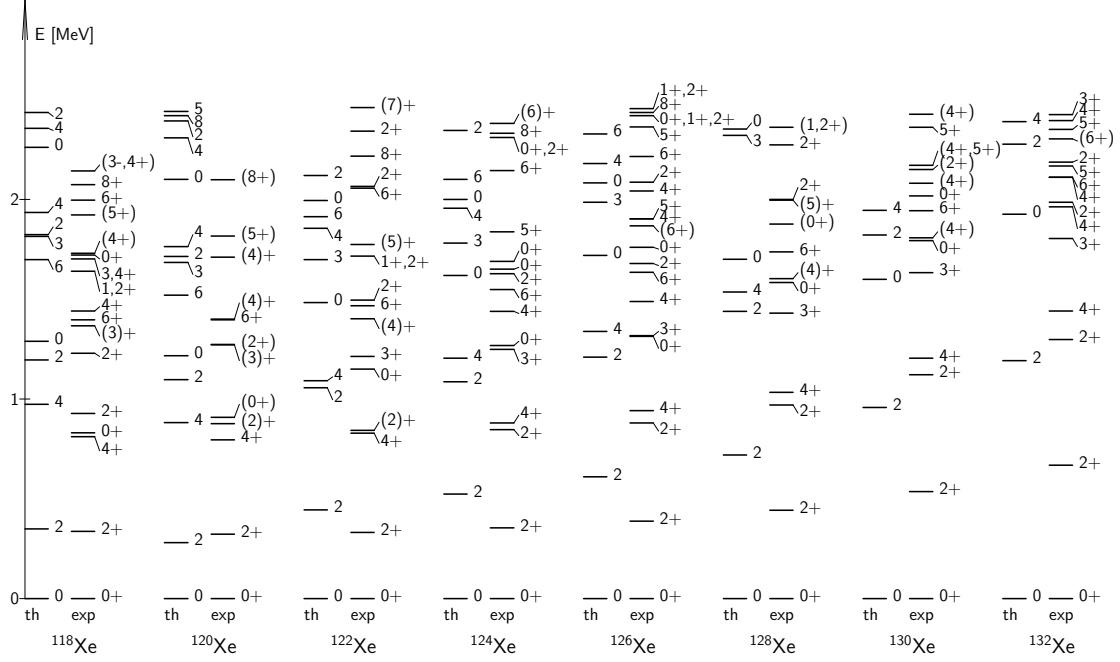


Fig. 8: The same as in Fig. 4 but for xenon isotopes  $^{118-132}\text{Xe}$ .

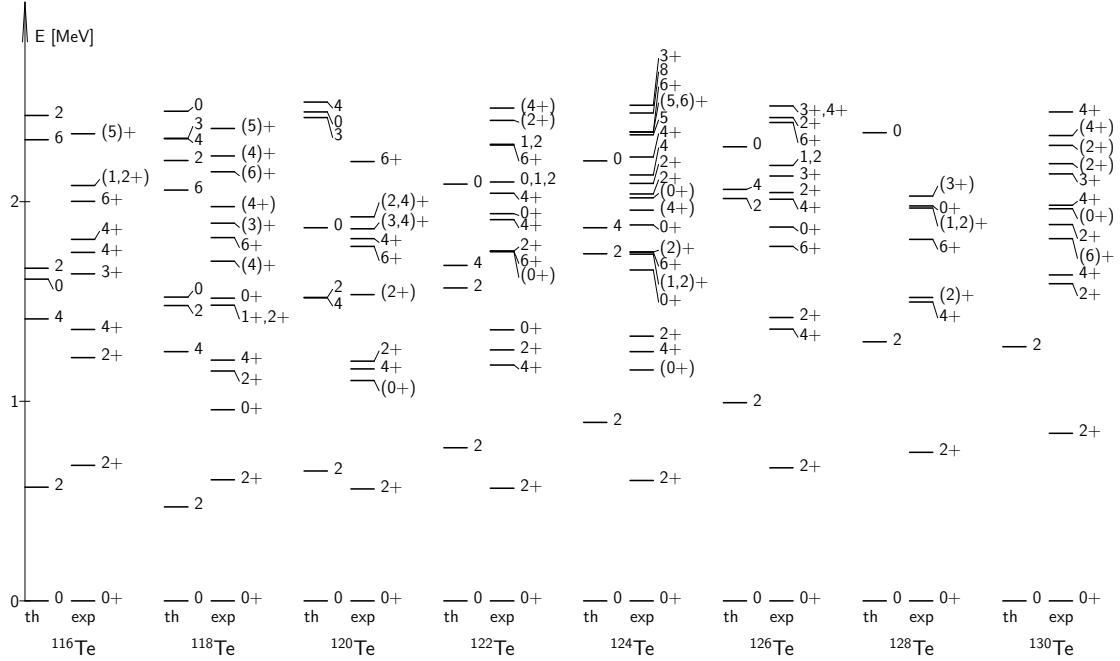


Fig. 9: The same as in Fig. 4 but for tellurium isotopes  $^{116-130}\text{Te}$ .

$^{124}\text{Ce}$ ,  $^{126}\text{Ce}$  and  $^{128}\text{Ce}$  while the first  $2^+$  state becomes too high for heavier isotopes. In the case of two heaviest ones,  $^{136}\text{Ce}$  and  $^{138}\text{Ce}$ , also two-phonon triplet of states  $0^+$ ,  $2^+$ ,  $4^+$  is visibly too high (Fig. 6). The spectra only of two or three lightest isotopes of barium, xenon and tellurium,  $^{122}\text{Ba}$ ,  $^{124}\text{Ba}$ ,  $^{126}\text{Ba}$ ,  $^{118}\text{Xe}$ ,  $^{120}\text{Xe}$ ,  $^{116}\text{Te}$ ,  $^{118}\text{Te}$ , are of a good energy

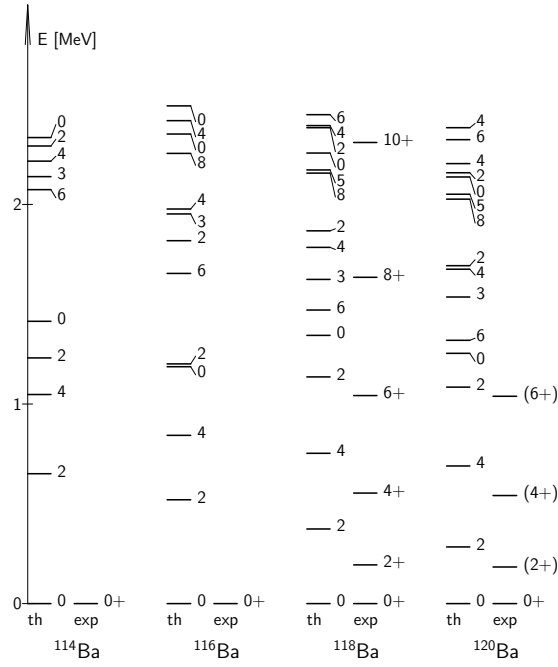


Fig. 10: The same as in Fig. 4 but for light barium isotopes  $^{114-120}\text{Ba}$ . Experimental data for  $^{118}\text{Ba}$  are taken from [45].

scale. For the heavier isotopes the calculation gives too stretched energy spectra (Figs 7, 8 and 9). The theoretical energy levels for very light barium isotopes  $^{114-120}\text{Ba}$  are plotted additionally in Fig 10. The results for  $^{118}\text{Ba}$  are compared with very recent experimental data from Ref. [45]. Here the energy scale of the theoretical results for  $^{118}\text{Ba}$  and  $^{120}\text{Ba}$  seems also to be too stretched with respect to the experimental tendency. Probably the same occurs for unknown yet levels in  $^{114}\text{Ba}$  and  $^{116}\text{Ba}$  which have recently been investigated for the first time [46].

## 6.2 The electromagnetic properties

The results of calculation of the reduced transition probability from the first excited  $2^+$  state to the ground state,  $B(E2; 2^+ \rightarrow 0^+)$  are compared with experimental data in Fig. 11. It is seen that the  $B(E2)$  values for isotopes of Ce, Nd and Sm are reproduced quite well. The calculated probabilities for most cases of the Xe and Ba isotopes are only a little too large and a tendency to decrease probabilities with increase the neutron number is reproduced correctly. An agreement of the theory with experiment is, in general, better for heavier Xe and Ba isotopes and worse for lighter ones. A similar observation can be made for tellurium isotopes. However, the theory gives  $B(E2)$  values plainly too big in this case although the tendency of changes from isotope to isotope is again correct.

Theoretical values of the spectroscopic quadrupole moment of the first  $2^+$  state are shown in Fig. 12. The experimental data are scanty for this quantity and it is difficult to estimate of agreement between calculations and measurements. In cases of  $^{130}\text{Ba}$  and  $^{134}\text{Ba}$  it is very good. An opposite sign of the quadrupole moment is predicted for  $^{136}\text{Ba}$ . For the Te isotopes the agreement is rather poor.

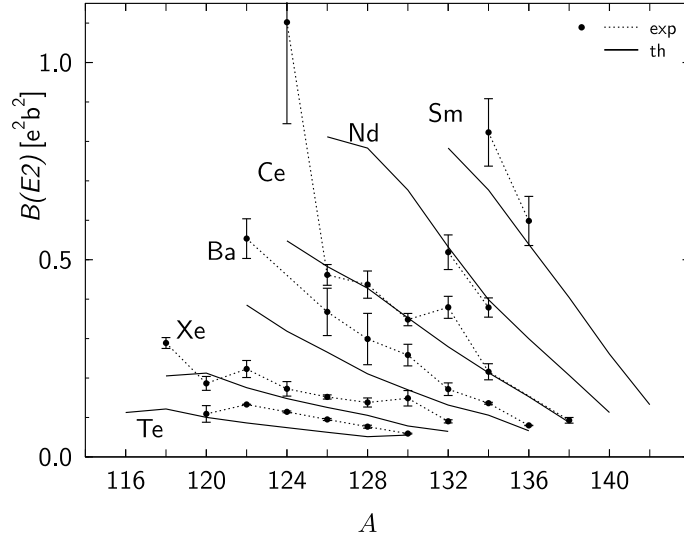


Fig. 11: Calculated and experimental [44] reduced transition probabilities  $B(E2; 2^+ \rightarrow 0^+)$  (in  $e^2b^2$ ) from the first excited  $2^+$  state to the ground state.

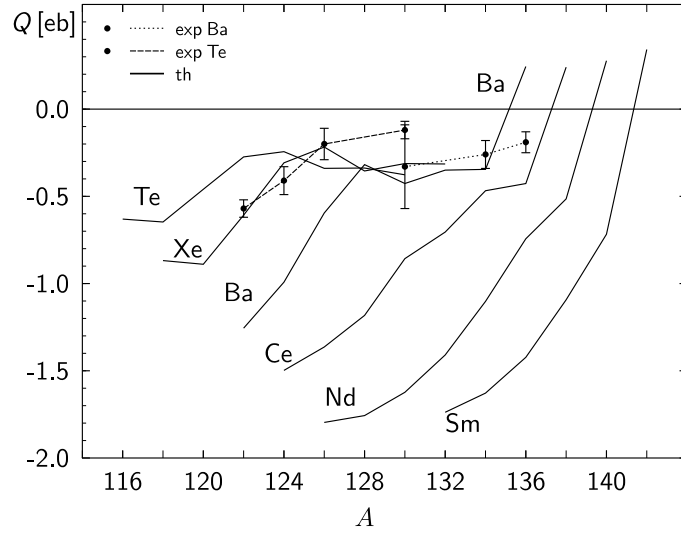


Fig. 12: Calculated and experimental [44] spectroscopic electric quadrupole moments (in eb) of the first excited  $2^+$  state.

The calculated magnetic dipole moments agree with the experimental values in all of known cases of the Xe, Ba and Nd isotopes. The agreement between the theory and

experiment for the tellurium isotopes is again poorer. This is shown in Fig. 13.

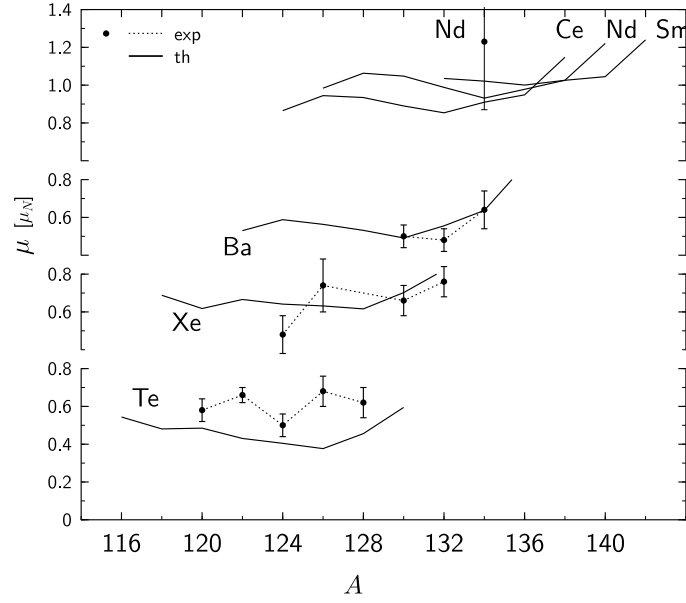


Fig. 13: Calculated and experimental [44] magnetic dipole moments (in  $\mu_N$ ) of the first excited  $2^+$  state.

Fig. 14 shows the results of calculation of isotopic shifts for the charge root mean square radii. The experimental values in all of cases available for the Xe and Ba isotopes [47] are reproduced very well.

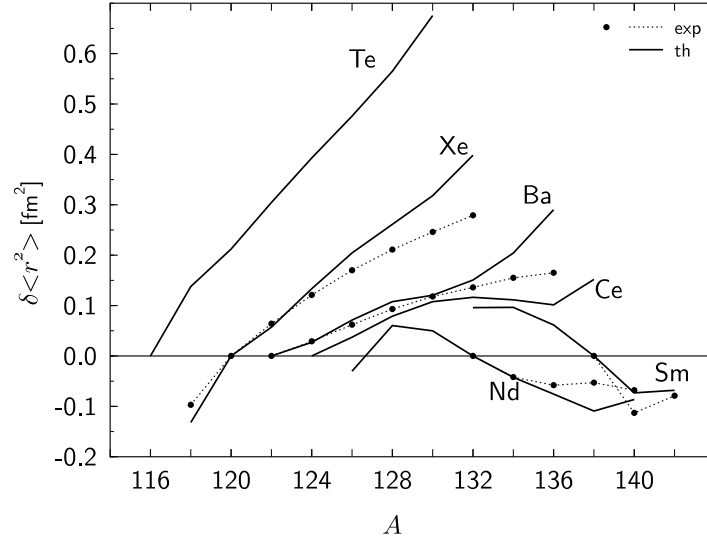


Fig. 14: Calculated and experimental [47] isotopic shifts of the mean square radii in the ground states.

The knowledge of experimental data for other electromagnetic properties like transition probabilities from higher excited states, branching and mixing ratios is still rather poor in the investigated region of nuclear chart and, therefore, we do not discuss them here.

## 7 Conclusions

The low-lying quadrupole collective states of 48 even-even nuclei from the region  $50 < Z, N < 82$  of the chart of nuclides are investigated within the framework of the generalized Bohr Hamiltonian. The collective potential and inertial functions are determined microscopically. There are no free parameters in the calculation. Taking the coupling of the quadrupole and pairing vibrations into account brings the energy levels down to the scale comparable with that of experimental one. In general, the GBH works better in the case of elements with larger  $Z$ , namely, Ce, Nd and Sm than for Xe, Ba and, especially, Te which has only two protons outside the closed shell  $Z = 50$ . Energies are better reproduced by the calculation for isotopes with lower number of neutrons. For those with neutron number  $N = 78, 80$  the energy levels are, as a rule, too high. On the contrary, electromagnetic properties seem to be better reproduced just in the case of heavier isotopes. The calculated reduced probability of the  $2^+ \rightarrow 0^+$  transition, if not reproduced well, has a tendency to be too large, especially in cases of lighter isotopes for which energy levels lie in more or less correct position.

It does not make sense to discuss how good or how bad are our results obtained with no free parameters in comparison to those of other approaches in which some parameters are usually fitted to the data.

Finally, we may say that though the collective model based on the generalized Bohr Hamiltonian gives qualitatively reasonable results for nuclei from the major shell  $50 < Z, N < 82$ , it is not able to reproduce all of collective characteristics simultaneously in detail. We think that dynamical effects of coupling with pairing vibrations can improve the description of collective states in question.

## Appendix.

### Symmetrization under the O group

All of transformations which change names and senses of the intrinsic axes and form the octahedral group O can be expressed through the three well known Bohr rotations,  $R_1, R_2, R_3$  (see refs [1, 2, 3, 24] for their definition). Therefore, it is sufficient to symmetrize functions  $\varphi_{Lm}^{IM}(\beta, \gamma, \Omega)$  of eq. (10) with respect to  $R_i$ , ( $i = 1, 2, 3$ ). Symmetrization under  $R_1$  and  $R_2$  gives

$$(1+R_1)(1+R_2+R_2^2+R_2^3)\varphi_{Lmn}^{IM}(\beta, \gamma, \Omega) \propto \psi_{Lmn}^{IM}(\beta, \gamma, \Omega) = e^{-\mu\beta^2/2}\beta^n p_{Lm}(\gamma)\Phi_{ML}^I(\Omega) \quad (35)$$

where

$$p_{Lm}(\gamma) = \begin{cases} \cos m\gamma & \text{for } L/2 \text{ even,} \\ \sin m\gamma & \text{for } L/2 \text{ odd} \end{cases} \quad (36)$$



and  $\Phi_{ML}^I$  is given by eq. (12). The additional symmetrization under  $R_3$  leads to the functions:

$$(1 + R_3 + R_3^2)\psi_{Lmn}^{IM}(\beta, \gamma, \Omega) = \Psi_{Lmn}^{IM}(\beta, \gamma, \Omega) = e^{-\mu\beta^2/2}\beta^n \sum_{K=\text{even} \geq 0} f_{LmK}^I(\gamma) \Phi_{MK}^I(\Omega) \quad (37)$$

where

$$f_{LmK}^I(\gamma) = c_{LmK}^I p_{Km}(\gamma). \quad (38)$$

Coefficients  $c_{LmK}^I$  are equal to

$$c_{LmK}^I = \delta_{LK} + 2(-1)^{K/2}[(1 + \delta_{L0})(1 + \delta_{K0})]^{-1/2} d_{KL}^I(\pi/2) a_{LmK},$$

$$a_{LmK} = \begin{cases} 2 \cos(2m\pi/3) & \text{for } (K + L)/2 \text{ even,} \\ 2 \sin(2m\pi/3) & \text{for } K/2 \text{ even, } L/2 \text{ odd,} \\ -2 \sin(2m\pi/3) & \text{for } K/2 \text{ odd, } L/2 \text{ even.} \end{cases} \quad (39)$$

Function  $d_{KL}^I(\theta)$  is related to the Wigner function in a usual way:  $D_{KL}^I(\phi, \theta, \psi) = e^{iK\phi} d_{KL}^I(\theta) e^{iL\psi}$ .

Since  $R_3$  does not commute with  $R_1$  and  $R_2$  the set of functions of eq. (37) is linear dependent. Selection of linear independent functions from the set (37) leads to restrictions on values of quantum the number  $L$  for given  $I$  and  $m$ . The number  $L$  takes even integer values ranging from  $2\delta_{I\text{odd}} = 2(1 - \delta_{I\text{even}})$  to  $L_{\text{max}}^I(m)$ , where  $\delta_{I\text{even}}$  is equal to 1 for an even  $I$  and 0 for an odd one, and

$$L_{\text{max}}^I(m) = \begin{cases} 2 \cdot [I/12] + 2\Delta_I - 2\delta_{I\text{even}} & \text{for } m = 0, \\ 2 \cdot [I/6] & \text{for } m > 0, I \bmod 3 = 1, \\ 2 \cdot [I/6] - 2\delta_{I\text{even}} & \text{for } m > 0, m \bmod 3 = 0, I \bmod 3 = 2, \\ & \text{or } m \bmod 3 \neq 0, I \bmod 3 = 0, \\ 2 \cdot [I/6] + 2\delta_{I\text{odd}} & \text{for } m > 0, m \bmod 3 = 0, I \bmod 3 = 0, \\ & \text{or } m \bmod 3 \neq 0, I \bmod 3 = 2, \end{cases} \quad (40)$$

with

$$\Delta_I = \begin{cases} 1 & \text{for } I \bmod 12 = 0, 4, 6, 8, 9, 10, \\ 0 & \text{for } I \bmod 12 = 1, 2, 3, 5, 7, 11. \end{cases} \quad (41)$$

A rational number  $N/M$  in square brackets,  $[N/M]$ , stands for its integer part.

We have to consider also the boundary conditions in  $\gamma$  (it is for  $\gamma = k\pi/3$ ). The combinations of the linear independent functions  $\Psi_{Lmn}^{IM}$  which fulfill these conditions and, thus, form a (nonorthogonal) basis in the domain of the Bohr Hamiltonian, are (cf. [35]):

$$\tilde{\Psi}_{Lmn}^{IM}(\beta, \gamma, \Omega) = e^{-\mu\beta^2/2}\beta^n \sum_{K=\text{even} \geq 0} \tilde{f}_{LmK}^I(\gamma) \Phi_{MK}^I \quad (42)$$

where  $\tilde{f}_{LmK}^I$  are the following combinations of functions  $f_{LmK}^I$  of eq. (38) for all possible

values of  $K$ :

$$\begin{aligned}
& \underline{m < 6} \\
& \begin{aligned}
\tilde{f}_{00K}^I &= f_{00K}^I \\
\tilde{f}_{02K}^I &= f_{02K}^I + \frac{1}{2}f_{00K}^I \\
\tilde{f}_{L3K}^I &= f_{L3K}^I + 2\delta_{L0}f_{01K}^I & \text{for } L = (0), 2, 6, 10, \dots, 4 \cdot [(L_{\max}^I(3) + 2)/4] - 2 \\
\tilde{f}_{L4K}^I &= f_{L4K}^I - (-1)^{L/2}f_{L2K}^I & \text{for } L = (0), 2, 4, \dots, L_{\max}^I(2) \\
\tilde{f}_{L5K}^I &= f_{L5K}^I - (-1)^{L/2}f_{L1K}^I & \text{for } L = (0), 2, 4, \dots, L_{\max}^I(1)
\end{aligned} \\
& \underline{m \geq 6} \\
& \begin{aligned}
m \bmod 3 &\neq 0 \\
\tilde{f}_{LmK}^I &= f_{LmK}^I - f_{Lm-6K}^I & \text{for } L = (0), 2, 4, \dots, L_{\max}^I(m) \\
m \bmod 3 &= 0 \\
\tilde{f}_{LmK}^I &= f_{LmK}^I - \delta_{L \bmod 40}f_{Lm-6K}^I & \text{for } L = (0), 2, 4, \dots, L_{\max}^I(m)
\end{aligned}
\end{aligned} \tag{43}$$

where the lowest value of  $L$  in parentheses is omitted for odd  $I$ 's.

The orthonormal (with respect to the measure  $d\tau_0$ ) set of functions reads:

$$\tilde{F}_{Lmn}^{IM}(\beta, \gamma, \Omega) = e^{-\mu\beta^2/2} R_{nm}(\beta; \mu) \tilde{T}_{Lm}^{IM}(\gamma, \Omega) \tag{44}$$

where

$$\tilde{T}_{Lm}^{IM}(\gamma, \Omega) = \sum_K \sum_{L'm'} E_{Lm, L'm'}^{(Ip)} \tilde{f}_{L'm'K}^I(\gamma) \Phi_{MK}^I(\Omega) \tag{45}$$

and

$$R_{nm}(\beta; \mu) = \sum_{n'} S_{nn'}^{(m)}(\mu) \beta^{n'} \tag{46}$$

Lower diagonal matrices  $S^{(m)}(\mu)$  and  $E^{(p)}$  are obtained through Cholesky-Banachiewicz method. The running index  $m'$  in eq. (45) has the same parity  $p$  as that of  $m$ . So, we have two matrices  $E^{(Ip)}$ , one for each parity, for a given  $I$ . On the other hand, matrices  $S^{(m)}(\mu)$  depend on  $m$  itself. They depend also on parameter  $\mu$ . However, it turns out that

$$R_{nm}(\beta; \mu) = \mu^{5/2} R_{nm}(\mu\beta; \mu=1) \tag{47}$$

Hence, it is sufficient to perform the orthonormalization only once.

Hamiltonian  $\hat{\mathcal{H}}_{\text{coll}}$  is hermitian with the measure  $d\tau$  of eq. (7). The basis orthonormal with respect to this measure is finally of the following form:

$$F_{Lmn}^{IM}(\beta, \gamma, \Omega) = (w(\beta, \gamma)r(\beta, \gamma))^{-1/4} \tilde{F}_{Lmn}^{IM}(\beta, \gamma, \Omega). \tag{48}$$

## Acknowledgement

This work was supported in part by the Polish Committee for Scientific Research under Contract No. 2 P03B 068 13.

# References

- [1] A. Bohr, Mat. Fys. Medd. Dan. Vid. Selsk. **26**, no. 14 (1952)
- [2] K. Kumar and M. Baranger, Nucl. Phys. **A92** (1967) 608
- [3] J. M. Eisenberg and W. Greiner, *Nuclear Models*, (North-Holland, Amsterdam, 1987)
- [4] T. Kaniowska, A. Sobiczewski, K. Pomorski and S. G. Rohoziński, Nucl. Phys. **A274** (1976) 151
- [5] S. G. Rohoziński, J. Dobaczewski, B. Nerlo-Pomorska, K. Pomorski and J. Srebrny, Nucl. Phys. **A292** (1977) 66
- [6] A. Gózdź, K. Pomorski, M. Brack and E. Werner, Nucl. Phys. **A442** (1985) 26
- [7] D. A. Arseniev, A. Sobiczewski and V. G. Soloviev, Nucl. Phys. **A126** (1969) 15
- [8] S. G. Rohoziński, J. Srebrny and K. Horbaczewska Z. Phys. **268** (1973) 401
- [9] J. Srebrny, T. Czosnyka, W. Karczmarczyk, P. Napiórkowski, Ch. Droste, H.-J. Wollersheim, H. Emling, H. Grein, R. Kulessa, D. Cline and C. Fahlander, Nucl. Phys. **A557** (1993) 663c
- [10] U. Meyer, A. Faessler and S. B. Khadkikar, Nucl. Phys. **A624** (1997) 391
- [11] A. Subber, W. D. Hamilton, P. Park, K. Kumar, J. Phys. **G13** (1987) 161
- [12] P. Petkov, A. Dewald and W. Andrejtscheff, Phys. Rev. **C51** (1995) 2511
- [13] E. Hammarén, K. W. Schmid, F. Grümmer, A. Faessler and B. Fladt, Nucl. Phys. **A454** (1986) 301
- [14] X.-W. Pan, J.-L. Ping, D. H. Feng, J.-Q. Chen, C.-L. Wu, M. W. Guidry, Phys. Rev. **C51** (1996) 715
- [15] R. Devi and S. K. Khosa, Z. Phys. **A354** (1996) 45
- [16] R. Devi, S. P. Sarswat, A. Bharti, S. K. Khosa, Phys. Rev. **C55** (1997) 2433
- [17] R. F. Casten and P. von Brentano, *Phys. Lett.* **B152** (1985) 22
- [18] G. Puddu, O. Scholten and T. Otsuka, *Nucl. Phys.* **A348** (1980) 109
- [19] T. Seo, Z. Phys. **A324** (1986) 43
- [20] A. Gózdź and K. Pomorski, Nucl. Phys. **A451** (1986) 1
- [21] S. G. Nilsson, C. F. Tsang, A. Sobiczewski, Z. Szymański, S. Wycech, C. Gustafson, I. L. Lamm, P. Möller and B. Nilsson, Nucl. Phys. **A131** (1969) 1
- [22] H. Sakamoto, Phys. Rev. **C52** (1995) 177
- [23] M. Hamermesh, *Group theory and its applications to physical problems* (Addison-Wesley, Reading, MA, 1962)
- [24] T. M. Corrigan, F. J. Margetan and S. A. Williams, Phys. Rev. **C14** (1976) 2279
- [25] D. Troltenier, J. A. Maruhn, W. Greiner and P. O. Hess, Z. Phys. **A343** (1992) 25
- [26] G. G. Dussel and D. R. Bes, Nucl. Phys. **A143** (1970) 623
- [27] G. Gneuss and W. Greiner, Nucl. Phys. **A171** (1971) 449
- [28] K. Kumar, Nucl. Phys. **A 231** (1974) 189
- [29] J. Libert and P. Quentin, Z. Phys. **A306** (1982) 315
- [30] E. Chacón, M. Moshinsky and R. Sharp, J. Math. Phys. **17** (1976) 668
- [31] E. Chacón and M. Moshinsky, J. Math. Phys. **18** (1977) 870
- [32] A. Gheorghe, A. A. Raduta and V. Ceaurescu, Nucl. Phys. **A296** (1978) 228

- [33] S. Szpikowski, and A. Gózdź; Nucl. Phys. **A340** (1980) 76
- [34] I. Deloncle, *These de doctorat de l'Universite Paris 6* (1989)
- [35] L. Próchniak, to be published
- [36] A. Ralston, *A first course in numerical analysis* (McGraw-Hill, New York, 1965)
- [37] S. Piłat, K. Pomorski and A. Staszczak, Z. Phys. **A332** (1989) 259
- [38] P. Möller, J. R. Nix, W. D. Myers and W. J. Swiatecki, At. Data Nucl. Data Tables **59** (1995) 185
- [39] A. Staszczak, K. Pomorski, A. Baran and K. Böning, Phys. Lett. **161B** (1985) 227
- [40] S. Piłat and K. Pomorski, Nucl. Phys. **A554** (1993) 413
- [41] D. R. Bès, R. A. Broglia, R. P. J. Perazzo and K. Kumar, Nucl. Phys. **A143** (1970) 1
- [42] A. Gózdź, K. Pomorski, M. Brack and E. Werner, Nucl. Phys. **A442** (1985) 50
- [43] J. Dobaczewski and S. G. Rohoziński, *Symmetries and Nuclear Structure*, Proc. International Research Symposium, Dubrovnik, 5–14 June 1986, ed. R. A. Meyer, V. Paar, (Harwood, Chur, 1987) p. 508
- [44] Data extracted using the NNDC On-Line Data Service from the ENSDF database, file revised as of 7th Nov 1997. M. Bhat, Evaluated Nuclear Structure Data File (ENSDF), Nuclear Data for Science and Technology, page 817, ed. by S. M. Qaim (Springer-Verlag, Berlin, Germany, 1992)
- [45] J. F. Smith *et al.*, Phys. Rev. **C57** (1998) R1037
- [46] Z. Janas *et al.*, Nucl. Phys. **A627** (1997) 119
- [47] E. Otten, Nuclear Radii and Moments of Unstable Isotope, in: *Treatise on Heavy-Ion Science*, Vol 8, ed. by D. A. Bromley, Plenum Press, New York (1989), pp. 517-638